IL NUOVO CIMENTO Vol. 33 C, N. 4 Luglio-Agosto 2010
DOI 10.1393/ncc/i2010-10658-1

Colloquia: TOP2010

Top quark pair production with two jets at next-to-leading order

M. Worek

Fachbereich C, Bergische Universität Wuppertal - D-42097 Wuppertal, Germany

(ricevuto il 19 Luglio 2010; approvato il 19 Luglio 2010; pubblicato online l'1 Ottobre 2010)

Summary. — A report on the recent next-to-leading order QCD calculations to $t\bar{t}b\bar{b}$ and $t\bar{t}jj$ at the CERN Large Hardon Collider is given. The elements of the calculation are briefly summarized and results for integrated and differential cross sections are presented.

PACS `12.38.Bx` – Perturbative calculations.
PACS `14.65.Ha` – Top quarks.

1. – Introduction

Even though first results for next-to-leading order (NLO) QCD corrections to heavy quark production were presented in the late 80's and early 90's [1-4] the topic of higher-order corrections to $t\bar{t}$ is still very active and far from complete. Our present level of understanding is very well summarized in experimental and theoretical reviews, see, *e.g.*, [5-7]. Recent progress in NLO [8, 9] and next-to-next-to leading order (NNLO) [10-18] calculations, as well as next-to-next-to-leading-log resummations (NNLL) [19-21] for inclusive $t\bar{t}$ hadroproduction is truly astonishing. The list for the more exclusive channels is just as impressive: NLO QCD corrections have been calculated for the $t\bar{t}H$ signal [22-27], where the Higgs boson has been treated as a stable particle. Most recently the factorisable QCD corrections to this process have been presented [28], where higher-order corrections to both production and decay of the Higgs boson into a $b\bar{b}$ pair have been calculated. Moreover, NLO QCD corrections to a variety of $2 \to 3$ backgrounds processes $t\bar{t}j$ [29-31], $t\bar{t}Z$ [32] and $t\bar{t}\gamma$ [33] have been obtained. Last but not least, the NLO QCD corrections to the $2 \to 4$ backgrounds processes such as $t\bar{t}b\bar{b}$ [34-37] and $t\bar{t}jj$ [38] have also recently been completed.

Both processes $pp \to t\bar{t}b\bar{b}$ and $pp \to t\bar{t}jj$ represent very important background reactions to searches at the LHC, in particular to $t\bar{t}H$ production, where the Higgs boson decays into a $b\bar{b}$ pair. A successful analysis of this particular production channel requires the knowledge of direct $t\bar{t}b\bar{b}$ and $t\bar{t}jj$ production at NLO in QCD [39]. In this contribution, a brief report on these computations is given.

2. – Theoretical framework

NLO QCD corrections have been calculated within the Helac-Nlo framework. It consists of Helac-Phegas [40-42], which has, on its own, already been extensively used and tested in phenomenological studies see, *e.g*, [43-46]. Helac-Phegas is a multi-purpose, tree-level event generator which is the only existing implementation of the algorithm based on Dyson-Schwinger equations. It can be used to efficiently obtain helicity amplitudes and total cross sections for arbitrary multiparticle processes in the Standard Model. The program can generate all processes with 10 or more final state particles with full off-shell and finite width effects taking into account naturally both, spin and color correlations. The integration over the fractions x_1 and x_2 of the initial partons is done via Parni [47].

Virtual corrections are obtained using the Helac-1Loop program [48], based on the Ossola-Papadopoulos-Pittau (OPP) reduction technique [49, 50] and the reduction code CutTools [51-53]. Moreover, OneLOop [48] library has been used for the evaluation of the scalar integrals. Reweighting techniques, and helicity and colour sampling methods are used in order to optimize the performance of our system. The OPP reduction at the integrand level takes advantage of the knowledge that the final answer for one-loop amplitudes can be expressed in terms of a basis of known 4−, 3−, 2− and 1−point scalar integrals: boxes, triangles, bubbles and tadpoles(1):

$$\mathcal{A} = \sum_i d_i I_i^4 + \sum_i c_i I_i^3 + \sum_i b_i I_i^2 + \sum_i a_i I_i^1 + \mathcal{R},$$

where $\mathcal{R}$ is the so-called rational part and d_i, b_i, c_i, a_i are coefficients which have to be derived. The OPP method aims at computing them directly avoiding any computationally intensive integral reduction.

The OPP reduction is based on a representation of the numerator of amplitudes, a polynomial in the integration momentum, in a basis of polynomials given by products of the functions in the denominators. Clearly, the cancellation of such terms with the actual denominators will lead to scalar functions with a lower number of denominators. By virtue of the proof provided by the Passarino-Veltman reduction [54], we will end up with a tower of four-point and lower functions, as mentioned before. The determination of the decomposition in the new basis proceeds recursively, by setting chosen denominators on-shell. This is where the OPP method resembles generalized unitarity [55-64]. For most recent applications see *e.g.* [65-70]. It is important to stress that, working around four dimensions, allows to compute the numerator function in four dimensions. The difference to the complete result is of order ϵ, and can therefore be determined *a posteriori* in a simplified manner [52, 53]. Since the calculation of the coefficients of the reduction requires the evaluation of the numerator function for a given value of the loop momentum,

(1) Tadpole integrals are present only when there are internal massive propagators.

the corresponding diagrams can be thought of as tree level (all momenta are fixed) graphs. To complete the analogy, one needs to choose a propagator and consider it as cut. At this point the original amplitude for an n particle process becomes a tree level amplitude for an $n+2$ particle process. The advantage is that its value can be obtained by a tree level automate such as Helac-Phegas. The bookkeeping necessary for a practical implementation is managed by a new software, Helac-1Loop.

The OPP method has already been successfully applied to a large number of processes, apart from already mentioned $t\bar{t}b\bar{b}$, $t\bar{t}H \to t\bar{t}b\bar{b}$ and $t\bar{t}jj$ also to the production of three vector bosons, namely ZZZ, W^+W^-Z, W^+ZZ and $W^+W^-W^+$ final states at the LHC [71] and to the calculation of one-loop QED corrections to the hard-bremsstrahlung process $e^-e^+\gamma$ at e^-e^+ colliders [72]. Recently the OPP-approach has been implemented in the another framework called Samurai [73], together with an extension which accommodate an implementation of the generalized d-dimensional unitarity-cuts technique.

The singularities from soft or collinear parton emission are isolated via dipole subtraction for NLO QCD calculations [74] using the formulation for massive quarks [75] and for arbitrary polarizations [76]. After combining virtual and real corrections, singularities connected to collinear configurations in the final state as well as soft divergencies in the initial and final states cancel for infrared-safe observables automatically. Singularities connected to collinear initial-state splittings are removed via factorization by PDF redefinitions. Calculations are performed with the help of the Helac-Dipoles software [76], which is a complete and publicly available automatic implementation of Catani-Seymour dipole subtraction and consists of phase space integration of subtracted real radiation and integrated dipoles in both massless and massive cases. The phase space restriction on the contribution of the dipoles as originally proposed in [77, 78] is also implemented. Two values of the unphysical cutoff are always considered; $\alpha_{\max} = 1$, which corresponds to the case when all dipoles are included, and $\alpha_{\max} = 0.01$. The independence of the final result from this cutoff is explicitly checked in all our results, both for the integrated cross section and for the differential distributions. Moreover, also in this part helicity sampling methods are used in order to speed up the calculation.

The cancellation of divergences between the real and virtual corrections is always verified. In addition, the numerical precision of the latter has been assured by using gauge invariance tests and use of quadruple precision. Let us emphasise that all parts are calculated fully numerically in a completely automatic manner.

Finally, the phase-space integration is performed with the multichannel Monte Carlo generator Phegas [41] and Kaleu [79].

3. – Results

We consider proton-proton collisions at the LHC with a center-of-mass energy of $\sqrt{s} = 14\,\mathrm{TeV}$. The mass of the top quark is set to be $m_t = 172.6\,\mathrm{GeV}$. We leave it on-shell with unrestricted kinematics. The jets are defined by at most two partons using the k_T algorithm with a separation $\Delta R = 0.8$, where $\Delta R = \sqrt{(y_1 - y_2)^2 + (\phi_1 - \phi_2)^2}$, $y_i = 1/2 \ln(E_i - p_{i,z})/(E_i + p_{i,z})$ being the rapidity and ϕ_i the azimuthal angle of parton i. Moreover, the recombination is only performed if both partons satisfy $|y_i| < 5$ (approximate detector bounds). We further assume for $t\bar{t}b\bar{b}$ ($t\bar{t}jj$) processes, that the jets are separated by $\Delta R = 0.8$ (1.0) and have $|y_{\rm jet}| < 2.5$ (4.5). Their transverse momentum is required to be larger than 20 (50) GeV, respectively. We consistently use the CTEQ6 set of parton distribution functions, *i.e.* we take CTEQ6L1 PDFs with a 1-loop running α_s in LO and CTEQ6M PDFs with a 2-loop running α_s at NLO.

TABLE I. – *Integrated cross section at LO and NLO for $t\bar{t}b\bar{b}$ production at the LHC. The two NLO results refer to different values of the dipole phase space cutoff $\alpha_{\max}$. The scale choice is $\mu_R = \mu_f = m_{\rm top}$.*

$\sigma^{\rm LO}$ (fb)	$\sigma^{\rm NLO}_{\alpha_{\max}=1}$ (fb)	$\sigma^{\rm NLO}_{\alpha_{\max}=0.01}$ (fb)
1489.2 ± 0.9	2642 ± 3	2636 ± 3

We begin our presentation of the final results of our analysis with a discussion of the total cross section. For the central value of the scale, $\mu_R = \mu_F = \mu_0 = m_t$, results for $t\bar{t}b\bar{b}$ production are summarized in table I whereas results for $t\bar{t}jj$ production in table II. From the above result one can obtain K factors,

$$K_{pp\to t\bar{t}b\bar{b}+X} = 1.77, \qquad K_{pp\to t\bar{t}jj+X} = 0.89.$$

In case of $pp \to t\bar{t}b\bar{b} + X$ corrections are large of the order of 77%. However, they can be reduced substantially, even down to -11%, either by applying additional cuts or by a better choice of factorization and renormalization scales as already suggested by Bredenstein *et al.* [37]. In case of $pp \to t\bar{t}jj + X$ we have obtained negative corrections of the order of 11%. In both cases a dramatic reduction of the scale uncertainty is observed while going from LO to NLO. The residual scale uncertainties of the NLO predictions for the irreducible background are at the 33% level, while for the reducible background the error obtained by scale variation is of the order of 11%. The scale dependence of the corrections for both processes is graphically presented in fig. 1.

While the size of the corrections to the total cross section is certainly interesting, it is crucial to study the corrections to the distributions. In fig. 2 the differential distributions for two observables, namely the invariant mass and transverse momentum of the two-b-jet system are depicted for the $pp \to t\bar{t}b\bar{b} + X$ process. Clearly, the distributions show the same large corrections, which turn out to be relatively constant contrary to the quark induced case [34]. In fig. 3 the transverse momentum distributions of the hardest and second hardest jet are shown for the $pp \to t\bar{t}jj + X$ process. Distributions demonstrate tiny corrections up to at least 200 GeV, which means that the size of the corrections to the cross section is transmitted to the distributions. On the other hand, strongly altered shapes are visible at high p_T especially in case of the first hardest jet. Let us underline here that corrections to the high-p_T region can only be correctly described by higher-order calculations and are not altered by soft-collinear emissions simulated by parton showers.

TABLE II. – *Integrated cross section at LO and NLO for $t\bar{t}jj$ production at the LHC. The two NLO results refer to different values of the dipole phase space cutoff $\alpha_{\max}$. The scale choice is $\mu_R = \mu_f = m_{\rm top}$.*

$\sigma^{\rm LO}$ (pb)	$\sigma^{\rm NLO}_{\alpha_{\max}=1}$ (pb)	$\sigma^{\rm NLO}_{\alpha_{\max}=0.01}$ (pb)
120.17 ± 0.08	106.95 ± 0.17	106.56 ± 0.31

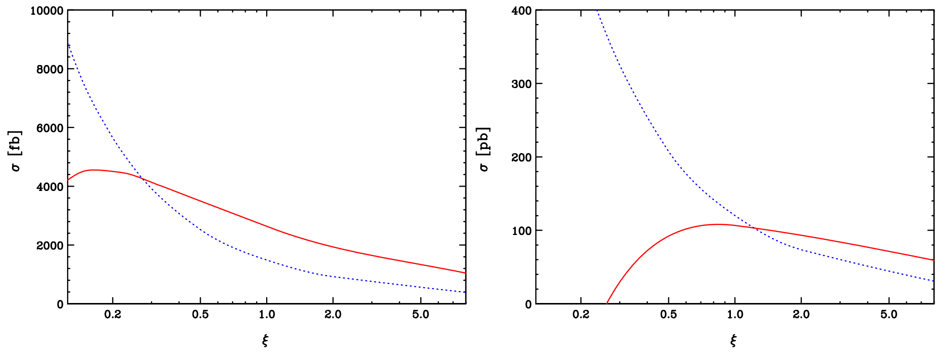

Fig. 1. – (Colour on-line) Scale dependence of the total cross section for $pp \to t\bar{t}b\bar{b} + X$ (left panel) and for $pp \to t\bar{t}jj + X$ (right panel) at the LHC with $\mu_R = \mu_F = \xi \cdot \mu_0$ where $\mu_0 = m_t =$ 172.6 GeV. The blue dotted curve corresponds to the LO whereas the red solid to the NLO one.

4. – Conclusions

A brief summary of the calculations of NLO QCD corrections to the background processes $pp \to t\bar{t}b\bar{b} + X$ and $pp \to t\bar{t}jj + X$ at the LHC has been presented. They have been calculated with the help of the HELAC-NLO system.

The QCD corrections to the integrated cross section for the irreducible background are found to be very large, changing the LO results by about 77%. The distributions show the same large corrections which are relatively constant. The residual scale uncertainties of the NLO predictions are at the 33% level. On the other hand, the corrections to the reducible background with respect to LO are negative and small, reaching 11%. The error obtained by scale variation is of the same order. The size of the corrections to the

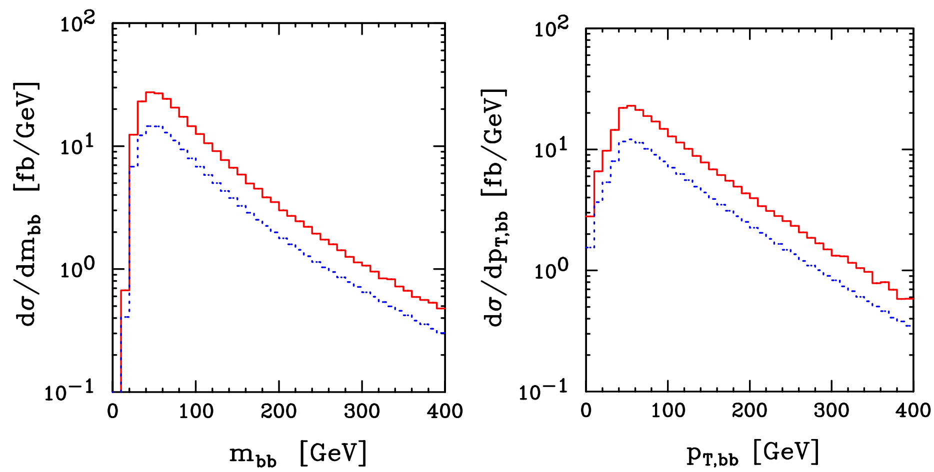

Fig. 2. – (Colour on-line) Distribution of the invariant mass $m_{b\bar{b}}$ (left panel) and the distribution in the transverse momentum $p_{T_{b\bar{b}}}$ (right panel) of the bottom-anti-bottom pair for $pp \to t\bar{t}b\bar{b}+X$ at the LHC. The blue dotted curve corresponds to the LO whereas the red solid to the NLO one.

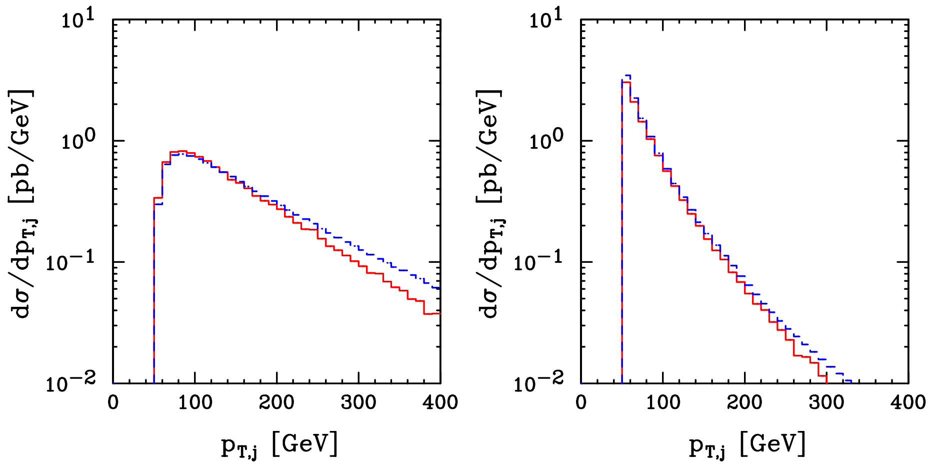

Fig. 3. – (Colour on-line) Distribution in the transverse momentum p_{T_j} of the 1st hardest jet (left panel) and the 2nd hardest jet (right panel) for $pp \to t\bar{t}jj + X$ at the LHC. The blue dotted curve corresponds to the LO whereas the red solid to the NLO one.

cross section is transmitted to the distributions at least for the low-p_T region. However, the shapes change appreciably at high p_T.

* * *

I would like to thank the organizers for the kind invitation and very pleasant atmosphere during the conference. The work presented here was funded by the Initiative and Networking Fund of the Helmholtz Association, contract HA-101 ("Physics at the Terascale") and by the RTN European Programme MRTN-CT-2006-035505 Heptools - Tools and Precision Calculations for Physics Discoveries at Colliders.

REFERENCES

[1] Nason P., Dawson S. and Ellis R. K., *Nucl. Phys. B*, **303** (1988) 607.
[2] Beenakker W., Kuijf H., van Neerven W. L. and Smith J., *Phys. Rev. D*, **40** (1989) 54.
[3] Nason P., Dawson S. and Ellis R. K., *Nucl. Phys. B*, **327** (1989) 49.
[4] Beenakker W., van Neerven W. L., Meng R., Schuler G. A. and Smith J., *Nucl. Phys. B*, **351** (1991) 507.
[5] Cacciari M., Frixione S., Mangano M. L., Nason P. and Ridolfi G., *JHEP*, **09** (2008) 127.
[6] Bernreuther W., *J. Phys. G*, **35** (2008) 083001.
[7] Incandela J. R., Quadt A., Wagner W. and Wicke D., *Prog. Part. Nucl. Phys.*, **63** (2009) 239.
[8] Melnikov K. and Schulze M., *JHEP*, **08** (2009) 049.
[9] Czakon M. and Mitov A., *Nucl. Phys. B*, **824** (2010) 111.
[10] Czakon M., Mitov A. and Moch S., *Phys. Lett. B*, **651** (2007) 147.
[11] Czakon M., Mitov A. and Moch S., *Nucl. Phys. B*, **798** (2008) 210.
[12] Korner J. G., Merebashvili Z. and Rogal M., *Phys. Rev. D*, **77** (2008) 094011.
[13] Czakon M., *Phys. Lett. B*, **664** (2008) 307.

[14] Bonciani R., Ferroglia A., Gehrmann T., Maitre D. and Studerus C., *JHEP*, **07** (2008) 129.
[15] Anastasiou C. and Aybat S. M., *Phys. Rev. D*, **78** (2008) 114006.
[16] Kniehl B., Merebashvili Z., Korner J. G. and Rogal M., *Phys. Rev. D*, **78** (2008) 094013.
[17] Bonciani R., Ferroglia A., Gehrmann T. and Studerus C., *JHEP*, **08** (2009) 067.
[18] Beneke M., Czakon M., Falgari P., Mitov A. and Schwinn C., *Phys. Lett. B*, **690** (2010) 483.
[19] Czakon M. and Mitov A., *Phys. Lett. B*, **680** (2009) 154.
[20] Beneke M., Falgari P. and Schwinn C., *Nucl. Phys. B*, **828** (2010) 69.
[21] Czakon M., Mitov A. and Sterman G. F., *Phys. Rev. D*, **80** (2009) 074017.
[22] Beenakker W. *et al.*, *Phys. Rev. Lett.*, **87** (2001) 201805.
[23] Reina L., Dawson S. and Wackeroth D., *Phys. Rev. D*, **65** (2002) 053017.
[24] Reina L. and Dawson S., *Phys. Rev. Lett.*, **87** (2001) 201804.
[25] Beenakker W. *et al.*, *Nucl. Phys. B*, **653** (2003) 151.
[26] Dawson S., Orr L. H., Reina L. and Wackeroth D., *Phys. Rev. D*, **67** (2003) 071503.
[27] Dawson S., Jackson C., Orr L. H., Reina L. and Wackeroth D., *Phys. Rev. D*, **68** (2003) 034022.
[28] Andersen J. R. *et al.*, arXiv:1003.1241 [hep-ph].
[29] Dittmaier S., Uwer P. and Weinzierl S., *Phys. Rev. Lett.*, **98** (2007) 262002.
[30] Dittmaier S., Uwer P. and Weinzierl S., *Eur. Phys. J. C*, **59** (2009) 625.
[31] Melnikov K. and Schulze M., arXiv:1004.3284 [hep-ph].
[32] Lazopoulos A., McElmurry T., Melnikov K. and Petriello F., *Phys. Lett. B*, **666** (2008) 62.
[33] Peng-Fei D. *et al.*, arXiv:0907.1324 [hep-ph].
[34] Bredenstein A., Denner A., Dittmaier S. and Pozzorini S., *JHEP*, **08** (2008) 108.
[35] Bredenstein A., Denner A., Dittmaier S. and Pozzorini S., *Phys. Rev. Lett.*, **103** (2009) 012002.
[36] Bevilacqua G., Czakon M., Papadopoulos C. G., Pittau R. and Worek M., *JHEP*, **09** (2009) 109.
[37] Bredenstein A., Denner A., Dittmaier S. and Pozzorini S., *JHEP*, **03** (2010) 021.
[38] Bevilacqua G., Czakon M., Papadopoulos C. G. and Worek M., *Phys. Rev. Lett.*, **104** (2010) 162002.
[39] Aad G. *et al.*, arXiv: 0901.0512 [hep-ex], CERN-OPEN-2008-020.
[40] Kanaki A. and Papadopoulos C. G., *Comput. Phys. Commun.*, **132** (2000) 306.
[41] Papadopoulos C. G., *Comput. Phys. Commun.*, **137** (2001) 247.
[42] Cafarella A., Papadopoulos C. G. and Worek M., *Comput. Phys. Commun.*, **180** (2009) 1941.
[43] Gleisberg T., Krauss F., Papadopoulos C. G., Schaelicke A. and Schumann S., *Eur. Phys. J. C*, **34** (2004) 173.
[44] Papadopoulos C. G. and Worek M., *Eur. Phys. J. C*, **50** (2007) 843.
[45] Alwall J. *et al.*, *Eur. Phys. J. C*, **53** (2008) 473.
[46] Englert C., Jager B., Worek M. and Zeppenfeld D., *Phys. Rev. D*, **80** (2009) 035027.
[47] van Hameren A., *Acta Phys. Polon. B*, **40** (2009) 259.
[48] van Hameren A., Papadopoulos C. G. and Pittau R., *JHEP*, **09** (2009) 106.
[49] Ossola G., Papadopoulos C. G. and Pittau R., *Nucl. Phys. B*, **763** (2007) 147.
[50] Pittau R., arXiv:1006.3773 [hep-ph].
[51] Ossola G., Papadopoulos C. G. and Pittau R., *JHEP*, **03** (2008) 042.
[52] Draggiotis P., Garzelli M. V., Papadopoulos C. G. and Pittau R., *JHEP*, **04** (2009) 072.
[53] Garzelli M. V., Malamos I. and Pittau R., *JHEP*, **01** (2010) 040.
[54] Passarino G. and Veltman M. J. G., *Nucl. Phys. B*, **160** (1979) 151.
[55] Bern Z., Dixon L. J., Dunbar D. C. and Kosower D. A., *Nucl. Phys. B*, **425** (1994) 217.

[56] Bern Z., Dixon L. J., Dunbar D. C. and Kosower D. A., *Nucl. Phys. B*, **435** (1995) 59.
[57] Witten E., *Commun. Math. Phys.*, **252** (2004) 189.
[58] Britto R., Cachazo F. and Feng B., *Nucl. Phys. B*, **725** (2005) 275.
[59] Anastasiou C., Britto R., Feng B., Kunszt Z. and Mastrolia P., *Phys. Lett. B*, **645** (2007) 213.
[60] Anastasiou C., Britto R., Feng B., Kunszt Z. and Mastrolia P., *JHEP*, **03** (2007) 111.
[61] Bern Z., Dixon L. J. and Kosower D. A., *Ann. Phys. (N.Y.)*, **322** (2007) 1587.
[62] Ellis R. K., Giele W. T. and Kunszt Z., *JHEP*, **03** (2008) 003.
[63] Giele W. T., Kunszt Z. and Melnikov K., *JHEP*, **04** (2008) 049.
[64] Ellis R. K., Giele W. T., Kunszt Z. and Melnikov K., *Nucl. Phys. B*, **822** (2009) 270.
[65] Berger C. F. *et al.*, *Phys. Rev. Lett.*, **102** (2009) 222001.
[66] Berger C. F. *et al.*, *Phys. Rev. D*, **80** (2009) 074036.
[67] Berger C. F. *et al.*, arXiv:1004.1659 [hep-ph].
[68] Ellis R. K., Melnikov K. and Zanderighi G., *JHEP*, **04** (2009) 077.
[69] Keith Ellis R., Melnikov K. and Zanderighi G., *Phys. Rev. D*, **80** (2009) 094002.
[70] Melnikov K. and Zanderighi G., *Phys. Rev.D*, **81** (2010) 074025.
[71] Binoth T., Ossola G., Papadopoulos C. G. and Pittau R., *JHEP*, **06** (2008) 082.
[72] Actis S., Mastrolia P. and Ossola G., *Phys. Lett. B*, **682** (2010) 419.
[73] Mastrolia P., Ossola G., Reiter T. and Tramontano F., arXiv:1006.0710 [hep-ph].
[74] Catani S. and Seymour M. H., *Nucl. Phys. B*, **485** (1997) 291.
[75] Catani S., Dittmaier S., Seymour M. H. and Trocsanyi Z., *Nucl. Phys. B*, **627** (2002) 189.
[76] Czakon M., Papadopoulos C. G. and Worek M., *JHEP*, **08** (2009) 085.
[77] Nagy Z. and Trocsanyi Z., *Phys. Rev. D*, **59** (1999) 014020.
[78] Nagy Z., *Phys. Rev. D*, **68** (2003) 094002.
[79] van Hameren A., arXiv:1003.4953 [hep-ph].